

# LUMINOSITY CORRELATIONS FOR GAMMA-RAY BURSTS AND IMPLICATIONS FOR THEIR PROMPT AND AFTERGLOW EMISSION MECHANISMS

J. SULTANA<sup>1</sup>, D. KAZANAS<sup>2</sup>, AND K. FUKUMURA<sup>2</sup>

<sup>1</sup> Mathematics Department, Faculty of Science, University of Malta, Msida MSD2080, Malta; joseph.sultana@um.edu.mt

<sup>2</sup> Astrophysics Science Division, NASA/Goddard Space Flight Center, Greenbelt, MD 20771, USA

Received 2012 May 12; accepted 2012 August 7; published 2012 September 24

## ABSTRACT

We present the relation between the ( $z$ - and  $k$ -corrected) spectral lags,  $\tau$ , for the standard *Swift* energy bands 50–100 keV and 100–200 keV and the peak isotropic luminosity,  $L_{\text{iso}}$  (a relation reported first by Norris et al.), for a subset of 12 long *Swift* gamma-ray bursts (GRBs) taken from a recent study of this relation by Ukwatta et al. The chosen GRBs are also a subset of the Dainotti et al. sample, a set of *Swift* GRBs of known redshift, employed in establishing a relation between the (GRB frame) luminosity,  $L_X$ , of the shallow (or constant) flux portion of the typical X-Ray Telescope GRB-afterglow light curve and the (GRB frame) time of transition to the normal decay rate,  $T_{\text{brk}}$ . We also present the  $L_X$ – $T_{\text{brk}}$  relation using only the bursts common in the two samples. The two relations exhibit a significant degree of correlation ( $\rho = -0.65$  for the  $L_{\text{iso}}$ – $\tau$  and  $\rho = -0.88$  for the  $L_X$ – $T_{\text{brk}}$  relation) and have surprisingly similar best-fit power-law indices ( $-1.19 \pm 0.17$  for  $L_{\text{iso}}$ – $\tau$  and  $-1.10 \pm 0.03$  for  $L_X$ – $T_{\text{brk}}$ ). Even more surprisingly, we noted that although  $\tau$  and  $T_{\text{brk}}$  represent different GRB time variables, it appears that the first relation ( $L_{\text{iso}}$ – $\tau$ ) extrapolates into the second one for timescales  $\tau \simeq T_{\text{brk}}$ . This fact suggests that these two relations have a common origin, which we conjecture to be kinematic. This relation adds to the recently discovered relations between properties of the prompt and afterglow GRB phases, indicating a much more intimate relation between these two phases than hitherto considered.

**Key words:** cosmological parameters – gamma-ray burst: general

**Online-only material:** color figures

## 1. INTRODUCTION

Gamma-ray bursts (GRBs) are extremely bright explosions with isotropic luminosities exceeding  $\sim 10^{54}$  erg s<sup>−1</sup>, durations in the range  $\sim 0.1$ –1000 s, and energy of peak luminosity in the  $\gamma$ -ray regime,  $E_p \sim 1$  MeV, hence their name. They are believed to originate in the collapse of stellar cores or the mergers of neutron stars, processes that result in jet-like relativistic outflows of Lorentz factors  $\Gamma \sim 300$ , whose kinetic energy is converted efficiently into radiation at distances  $r \sim 10^{15}$ – $10^{18}$  cm at a relativistic blast wave (RBW) to produce the observed events (for a review see Piran 2004). Following their most luminous, prompt,  $\gamma$ -ray emission, they shift into the afterglow phase with peak luminosity in the X-ray band and a duration of  $\sim 10^5$  s, in which their localization can be refined and optical detection can provide their redshift.

The theory of RBW slowdown indicated a smooth power-law decay  $\propto t^{-1}$  for the flux of their afterglow X-ray light curves, and indeed the pre-*Swift* sparsely sampled ones appeared consistent with such a behavior. However, their more densely sampled X-ray light curves with the X-Ray Telescope (XRT) aboard *Swift* uncovered significant deviations from this behavior. So, following the prompt emission in  $\gamma$ -rays, the typical XRT afterglow consists (Nousek et al. 2006) of a much steeper flux decline ( $\propto t^{-3}$  to  $t^{-6}$ ), followed by a  $10^2$ – $10^5$  s period of nearly constant flux, followed finally at  $t = T_{\text{brk}}$  by the more conventional power-law decline  $\propto t^{-1}$ . In addition, *Swift* follow-ups also discovered occasional flares on top of these light curves, as late as  $\sim 10^5$  s since the Burst Alert Telescope (BAT) trigger.

In their prompt phase GRBs exhibit a broad light-curve diversity and a large variance in their (estimated) RBW Lorentz factors ( $\Gamma \sim 100$ –1000). These properties, along with the non-thermal character of their spectra, suggest that at least in this phase, GRBs are not likely to provide well defined, underlying

systematics that would allow a probe of the physics of prompt emission. However, a number of correlations have been found between observables in the prompt phase (Riechart et al. 2001; Schaefer 2003; Ghirlanda et al. 2006; Amati et al. 2009), whose origin still remains largely unaccounted for.

One of the first such correlations, made possible only after the determination of the GRB redshifts by their afterglow emission, is that between the burst peak isotropic luminosity,  $L_{\text{iso}}$ , and the spectral lag,  $\tau$ , between different energy bands in the GRB spectrum. This relation has been studied in detail by a number of authors (Norris et al. 2000; Norris 2002; Gehrels et al. 2006; Schaefer 2007; Stamatikos 2008; Hakkila et al. 2008; Ukwatta et al. 2010, 2012; Wang et al. 2011) for data sets obtained by different instruments aboard different missions. The general conclusion of all these studies has been an anti-correlation  $L_{\text{iso}} \propto \tau^{-a}$  with a value of  $a \sim 0.77$ –1.8. The spectral lag is defined as the difference in the arrival time of high- and low-energy photons, and is taken to be positive when the time of arrival of high-energy photons precedes that of low-energy photons.

Normally, the spectral lag is extracted between two arbitrary energy bands in the observer frame and then corrected for the time dilatation effect ( $z$ -correction) by multiplying the lag value in the observer frame by  $(1+z)^{-1}$ . Moreover, the observed energy bands correspond to different energy bands at the GRB source frame for different redshifts, and so one needs to take into account this energy-dependent factor ( $k$ -correction). Using the assumption that the spectral lag is proportional to the pulse width, which in turn is proportional to the energy, Gehrels et al. (2006) approximately corrected for this effect by multiplying the lag value in the observer frame by  $(1+z)^{0.33}$ . Alternatively, the  $k$ -correction can be done by extracting the spectral lags in the GRB source frame. This is accomplished by choosing two energy bands in the source frame and then projecting these in the

observer frame using the relation  $E_{\text{obs}} = E_{\text{source}}/(1+z)$ , such that the projected energy bands lie in the *Swift* BAT energy range 15–350 keV. This alternative method of extracting the spectral lags in the source frame rather than the observer frame was recently used by Ukwatta et al. (2012) to obtain a similar result for the  $L_{\text{iso}} - \tau$  relation, but with a higher degree of correlation between the variables.

The physical origin of the lag–luminosity relation is still unclear. Some, including Salmonson (2000) and Ioka & Nakamura (2001), attributed this to a kinematic effect; Schaefer (2004), following an in-depth analysis of existing proposals, concludes in favor of the time evolution of the emitting electrons, on the basis of a correlation between the energy of the GRB peak emission and the burst’s instantaneous flux. However, irrespective of its physical origin, this relation is a useful tool in GRB science, not only for its use in distinguishing between long and short bursts (with long bursts in general exhibiting larger lags than short ones, although it has been shown (Gehrels et al. 2006; Hakkila et al. 2007) that this may not necessarily be true for every long GRB), but also for its implementation, together with other relations between GRB variables, in extending the Hubble diagram to higher redshifts (Schaefer 2007; Wang et al. 2011).

An altogether different correlation, pertaining to the GRB afterglow phase, has been reported recently by Dainotti et al. (2010). This work presents a correlation between the X-ray luminosity,  $L_X$ , of the plateau (or shallow decay) phase and the source frame break time  $T_{\text{brk}}$  in the XRT light curves of long GRBs. Using a sample of 62 *Swift* long GRBs, a correlation of the form  $\log L_X = \log a + b \log T_{\text{brk}}$ , with  $\log a = 51.06 \pm 1.02$  and  $b = -1.06^{+0.27}_{-0.28}$  was obtained. A similar but steeper correlation ( $b = -1.72^{+0.22}_{-0.21}$ ) was also obtained for a small group of GRBs which belong to the intermediate class (Norris & Bonnell 2006) between short and long ones, indicating that these may behave differently than the long GRBs. There have been claims (Cannizzo et al. 2011) that the Dainotti relation is just a selection effect due to the flux detection limit for *Swift*’s XRT which prevents clear observation of faint light curves from high redshift GRBs. This possibility was later investigated by Dainotti et al. (2011a) who showed that there is no systematic bias against faint plateaus at high  $z$ , thus confirming the existence of this relation. Moreover, Dainotti et al. (2011b) have obtained a number of significant correlations between the afterglow phase X-ray luminosity parameter  $L_X$  and prompt emission parameters such as the isotropic energy  $E_{\text{iso}}$ , peak energy  $E_{\text{peak}}$ , and the variability parameter  $V$  (Norris et al. 2000).

In this work we use a sample of 14 GRBs which are common in the Ukwatta et al. (2010) and Dainotti et al. (2010) studies, to obtain and compare their lag–luminosity and break-time–X-ray-luminosity relations in the GRB source frame after doing the necessary  $k$ - and  $z$ -corrections. The structure of the paper is as follows. In Section 2 we discuss briefly the correlations and computational procedures involved in the spectral-lag–isotropic-luminosity relation of Ukwatta et al. (2010) together with the X-ray luminosity of the GRB shallow afterglow phase and its break time from Dainotti et al. (2010). In Section 3 we present our results and then in Section 4 we summarize our findings and conclusions.

## 2. GRB DATA

In their work on the lag–luminosity relation, Ukwatta et al. (2010) developed a method for calculating the time-averaged spectral lag using a modification of the cross-correlation

function (CCF) with delay  $d$  (Band 1997) given by

$$\text{CCF}(d, x, y) = \frac{\sum_{i=\max(1, 1-d)}^{\min(N, N-d)} x_i y_{i+d}}{\sqrt{\sum_i x_i^2 \sum_i y_i^2}}, \quad (1)$$

where  $x_i$  and  $y_i$  are sets of time-sequenced data over  $N$  bins, and then defining the spectral lag as the time delay that corresponds to the global maximum of the CCF. They obtained the uncertainty in the spectral lag using the Monte Carlo method by simulating 1000 light curves for each real light-curve pair and calculating the CCF values using Equation (1) for a series of time delays. Then they obtained the uncertainty from the standard deviation of the CCF values per time delay bin of these simulated light curves.

To obtain the peak isotropic luminosity,  $L_{\text{iso}}$ , Ukwatta et al. (2010) fitted GRB spectra with the Band function (Band et al. 1993) for the photon flux per unit photon energy using

$$N(E) = \begin{cases} A \left( \frac{E}{100 \text{ keV}} \right)^\alpha e^{-(2+\alpha)E/E_{pk}}, & E \leq \left( \frac{\alpha-\beta}{2+\alpha} \right) E_{pk} \\ A \left( \frac{E}{100 \text{ keV}} \right)^\beta \left[ \frac{(\alpha-\beta)E_{pk}}{(2+\alpha)100 \text{ keV}} \right]^{\alpha-\beta} e^{(\beta-\alpha)}, & \text{otherwise,} \end{cases} \quad (2)$$

where  $A$  is the amplitude,  $\alpha$  and  $\beta$  are the low-energy and high-energy spectral indices, respectively, and  $E_{pk}$  is the peak energy of the  $\nu F_\nu$  spectrum. The observed peak flux is expressed in terms of the source frame spectrum  $N(E)$  between energies  $E_1 = 1.0$  keV and  $E_2 = 10000$  keV by

$$f_{\text{obs}} = \int_{E_1/(1+z)}^{E_2/(1+z)} N(E) E dE. \quad (3)$$

This was then used by Ukwatta et al. (2010) to compute the isotropic peak luminosity from

$$L_{\text{iso}} = 4\pi d_L^2 f_{\text{obs}}, \quad (4)$$

where  $d_L$  is the GRB luminosity distance computed in terms of the redshift  $z$  by

$$d_L = \frac{(1+z)c}{H_0} \int_0^z \frac{dz'}{\sqrt{\Omega_M(1+z')^3 + \Omega_\Lambda}}, \quad (5)$$

assuming a flat  $\Lambda$ CDM cosmological model with  $\Omega_M = 0.27$ ,  $\Omega_\Lambda = 0.73$ , and a Hubble constant  $H_0$  of  $70 \text{ km s}^{-1} \text{ Mpc}^{-1}$ . The uncertainty in  $L_{\text{iso}}$  was again determined using Monte Carlo methods by calculating the luminosity for 1000 variations in the spectral parameters in Equation (2) for each GRB, so that the real values and uncertainties are given by the sample means and sample standard deviations, respectively.

For the  $T_{\text{brk}}-L_X$  relation, Dainotti et al. (2010; see also Dainotti et al. 2008) used the fitting procedure of Willingale et al. (2007) to analyze the afterglow XRT light curves of a sample of *Swift* GRBs and derive the source frame parameters  $T_{\text{brk}}$  and  $L_X$  for each afterglow. The X-ray luminosity  $L_X$  at time  $T_{\text{brk}}$ , at which the light curve switches from the plateau to the declining phase, was calculated by using

$$L_X = \frac{4\pi d_L^2 F_X}{(1+z)^{1-\beta_a}}, \quad (6)$$

where  $d_L$  is the same luminosity distance given by Equation (5),  $F_X$  is the observed flux at time  $T_{\text{brk}}$ , and  $\beta_a$  is the spectral index obtained for each afterglow (Evans et al. 2009). Then they computed the uncertainties in the two parameters by using a Bayesian motivated technique by D’Agostini (2005).

**Table 1**  
GRB Redshift, Prompt, and Afterglow Parameters Taken from Ukwatta et al. (2010) and Dainotti et al. (2010)

| GRB        | Redshift | $E_{\text{pk}}^a$<br>(keV) | $L_{\text{iso}}$<br>(erg s $^{-1}$ )     | Lag<br>(ms)    | $\log L_X$<br>(erg s $^{-1}$ ) | $\log T_{\text{brk}}$<br>(s) |
|------------|----------|----------------------------|--|----------------|--------------------------------|------------------------------|
| GRB050401  | 2.899    | $119^{+16}_{-16}$          | $(1.38^{+0.16}_{-0.13}) \times 10^{53}$  | $106 \pm 118$  | $48.45 \pm 0.15$               | $3.28 \pm 0.14$              |
| GRB050603  | 2.821    | $349^{+18}_{-18}$          | $(6.32^{+0.47}_{-0.34}) \times 10^{53}$  | $20 \pm 18$    | $46.82 \pm 0.27$               | $4.25 \pm 0.25$              |
| GRB050922C | 2.199    | $[133^{+468}_{-39}]$       | $(5.17^{+28.00}_{-0.01}) \times 10^{52}$ | $19 \pm 72$    | $48.92 \pm 0.14$               | $2.08 \pm 0.07$              |
| GRB060206  | 4.056    | $75^{+12}_{-12}$           | $(6.28^{+2.50}_{-0.62}) \times 10^{52}$  | $-163 \pm 189$ | $48.65 \pm 0.14$               | $3.15 \pm 0.10$              |
| GRB060210  | 3.913    | $207^{+66}_{-47}$          | $(8.53^{+2.75}_{-0.92}) \times 10^{52}$  | $34 \pm 195$   | $47.90 \pm 0.24$               | $3.77 \pm 0.22$              |
| GRB060418  | 1.490    | $230^{+23}_{-23}$          | $(1.96^{+0.43}_{-0.13}) \times 10^{52}$  | $162 \pm 101$  | $47.85 \pm 0.11$               | $3.04 \pm 0.09$              |
| GRB060904B | 0.703    | $103^{+59}_{-26}$          | $(2.18^{+3.59}_{-0.32}) \times 10^{51}$  | $32 \pm 273$   | $46.53 \pm 0.28$               | $3.62 \pm 0.25$              |
| GRB060908  | 1.884    | $124^{+48}_{-24}$          | $(1.54^{+22.50}_{-0.22}) \times 10^{52}$ | $134 \pm 253$  | $48.24 \pm 0.12$               | $2.46 \pm 0.09$              |
| GRB061007  | 1.262    | $498^{+34}_{-30}$          | $(1.01^{+0.20}_{-0.08}) \times 10^{53}$  | $82 \pm 9$     | $49.39 \pm 0.04$               | $2.17 \pm 0.04$              |
| GRB061121  | 1.315    | $606^{+56}_{-45}$          | $(7.89^{+1.02}_{-0.47}) \times 10^{52}$  | $25 \pm 11$    | $48.35 \pm 0.10$               | $3.00 \pm 0.09$              |
| GRB070306  | 1.496    | $[76^{+131}_{-52}]$        | $(8.67^{+13.50}_{-0.27}) \times 10^{51}$ | $900 \pm 408$  | $47.07 \pm 0.05$               | $4.42 \pm 0.04$              |
| GRB071020  | 2.145    | $322^{+50}_{-33}$          | $(1.27^{+0.64}_{-0.15}) \times 10^{53}$  | $28 \pm 9$     | $49.22 \pm 0.08$               | $1.84 \pm 0.05$              |
| GRB080430  | 0.767    | $[67^{+85}_{-51}]$         | $(1.03^{+1.30}_{-0.07}) \times 10^{51}$  | $388 \pm 397$  | $46.03 \pm 0.08$               | $4.29 \pm 0.08$              |
| GRB080603B | 2.689    | $71^{+10}_{-10}$           | $(2.99^{+1.25}_{-0.30}) \times 10^{52}$  | $-172 \pm 56$  | $48.88 \pm 0.29$               | $2.92 \pm 0.24$              |

**Note.** <sup>a</sup> Values in brackets represent estimated values obtained using the method in Sakamoto et al. (2009).

### 3. RESULTS

We collected a sample of 14 long GRBs (i.e.,  $T_{90} > 2$  s) detected by *Swift*/BAT between 2005 and 2008 with known redshifts ranging from 0.703 (GRB 060904B) to 4.056 (GRB 060206), which are common in the samples of Ukwatta et al.'s (2010) and Dainotti et al.'s (2010) studies. The prompt and afterglow parameters of each GRB, including the spectral lag, peak isotropic luminosity  $L_{\text{iso}}$ , peak energy  $E_{\text{pk}}$ , break time  $T_{\text{brk}}$ , and X-ray luminosity  $L_X$  are shown in Table 1. The spectral lags are calculated between *Swift* energy bands 50–100 keV and 100–200 keV in the GRB source frame, after application of the  $z$ - and  $k$ -corrections, which are obtained by multiplying the observed values by  $(1+z)^{-0.67}$  as described in the section above. Two of the GRBs (GRB 060206 and GRB 080603B) have negative spectral lags, meaning that the time of arrival of low-energy photons precedes that of high-energy photons. Although negative lags are not necessarily unphysical (Ryde 2005), we chose to exclude them due to the logarithmic nature of the lag–luminosity relation in our plots. This was also done in previous studies of this relation by Ukwatta et al. (2010, 2012) and others.

We find that the  $z$ - and  $k$ -corrected spectral lag  $\tau$  and the peak isotropic luminosity  $L_{\text{iso}}$  are anti-correlated with a correlation coefficient  $\rho$  of  $-0.65$ , which is slightly weaker than the value of  $-0.73$  obtained by Ukwatta et al. (2010) for the whole sample of 31 GRBs. Figure 1 is a log–log plot of the isotropic peak luminosity versus the  $z$ - and  $k$ -corrected spectral lag with the following best-fit power-law curve<sup>3</sup>

$$\log L_{\text{iso}}(\text{erg s}^{-1}) = (54.87 \pm 0.29) - (1.19 \pm 0.17) \log((1+z)^{-0.67} \tau(\text{ms})). \quad (7)$$

The best-fit power-law index of  $-1.19 \pm 0.17$  is consistent with the earlier result ( $-1.4 \pm 0.1$ ) obtained by Ukwatta et al. (2010) for the full sample of 31 GRBs, with only redshift correction for

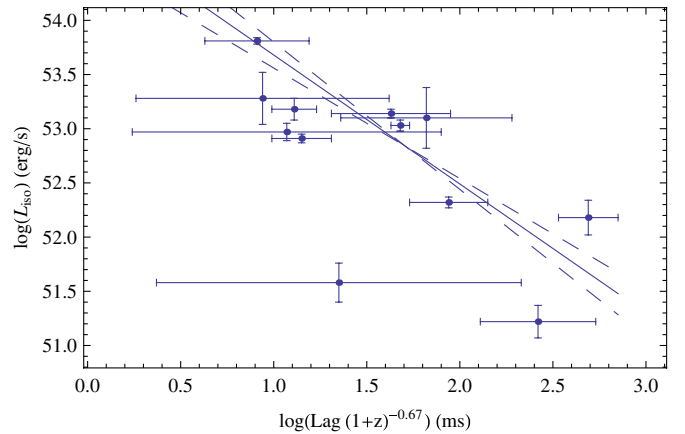


**Figure 1.** Log–log plot for the peak isotropic luminosity  $L_{\text{iso}}$  vs. source frame spectral lag between BAT channels (100–200 keV) and (50–100 keV).

(A color version of this figure is available in the online journal.)

the spectral lags. Our result also agrees with the  $-1.14$  power-law index obtained by Norris et al. (2000) using spectral lags between the BATSE energy bands 25–50 keV and 100–300 keV, and with those reported by Stamatikos (2008) ( $-1.16 \pm 0.21$ ) and Schaefer (2007) ( $-1.01 \pm 0.10$ ).

We have also obtained an anti-correlation with  $\rho = -0.88$  between the break time  $T_{\text{brk}}$  at the shallow-to-normal decay transition in the GRB afterglow light curve and the X-ray luminosity  $L_X$ . This is surprisingly stronger than the  $\rho = -0.76$  anti-correlation obtained by Dainotti et al. (2010) for the full sample of 62 long GRBs. Figure 2 shows a log–log plot of the break time  $T_{\text{brk}}$  versus the X-ray luminosity  $L_X$  in the GRB source frame, with a fitted power-law relation given by

$$\log L_X(\text{erg s}^{-1}) = (51.57 \pm 0.10) - (1.10 \pm 0.03) \log T_{\text{brk}}(\text{s}). \quad (8)$$

This best-fit power-law index is consistent with the value  $-1.06^{+0.27}_{-0.28}$  obtained by Dainotti et al. (2010) for the full sample of GRBs. It also agrees with the value obtained by Stratta et al. (2010) ( $\sim -1.07$ ) for a small sample of 12 long GRBs, and the

<sup>3</sup> The best-fit relations in this work were obtained by using the LinearFit function available in the *Experimental Data Analyst* package in Mathematica.

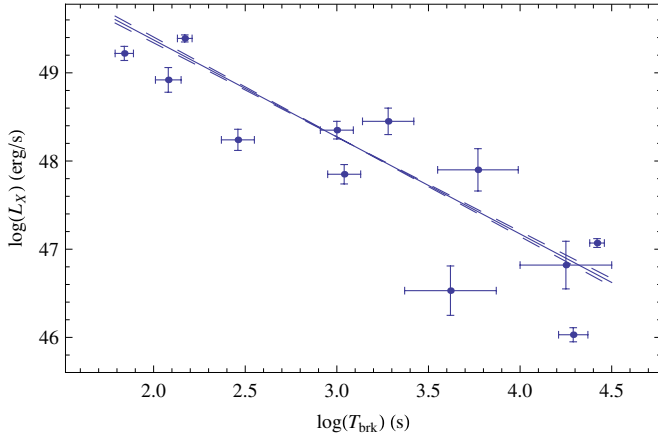


**Figure 2.** Log-log plot for the X-ray luminosity  $L_X$  vs. break time  $T_{\text{brk}}$ .  
(A color version of this figure is available in the online journal.)

recent study by Qi & Lu (2010) who also obtained a power-law index of  $(-0.89 \pm 0.19)$  for a sample of 47 GRBs.

Noting the similarity of the slopes of the two relations in Equations (7) and (8), and the fact that the ordinate of both is a luminosity while the abscissa represents a timescale, we present in Figure 3 a combined plot of the two relations in a single figure. It is evident, quite unexpectedly on our part, that one extrapolates into the other with the combined relation given by

$$\log L(\text{erg s}^{-1}) = (54.69 \pm 0.06) - (1.07 \pm 0.014) \log T(\text{ms}). \quad (9)$$

The increased dynamic range provides for a much tighter relation with a correlation coefficient  $\rho = -0.98$ , and with a slope much closer to  $-1$  than the individual relations.

#### 4. DISCUSSION AND CONCLUSION

In the sections above we reviewed correlations between the luminosities and timescales of two different stages in the GRB development, namely, the prompt emission and the shallow decay stage of their afterglow. We then reproduced the correlations between  $L-\tau$  for the prompt emission and  $L_X-T_{\text{brk}}$  for the afterglow, for the GRBs common in the data sets used by Ukwatta et al. (2010) and Dainotti et al. (2010), from the data already present in the literature. We have shown that although our GRB sample is small, both relations are consistent (in terms of power-law index and correlation coefficient) with the previous relations obtained using larger samples. Moreover, we have shown that these two relations extrapolate very well into each other and give a much tighter relation (Equation (9)) than the individual relations obtained so far.

For the first time we also noted that although the relations in Equations (7) and (8) represent different stages in the GRB evolution, their power-law indices are surprisingly similar. Yet from our data the source frame corrected spectral time lag and break time  $T_{\text{brk}}$  do not appear to be correlated. The fact that their normalizations are such that they extrapolate into each other, suggests that prompt and afterglow properties are interrelated. This fact could have been actually surmised from the original lag treatment of Norris et al. (2000) and the results of Dainotti et al. (2010). The reader can easily confirm that the relation of Norris et al. (2000) extrapolates into that of Dainotti et al. (2010). A correlation between the prompt and afterglow phases has also been explored by Salmonson & Galama (2002) who

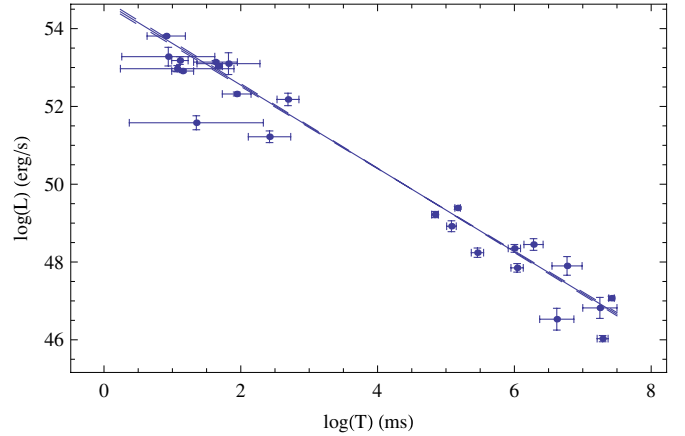


**Figure 3.** Log-log plot of the combined relations plotted in Figures 1 and 2 above with  $L_{\text{iso}}$  or  $L_X$  in the ordinate and the lag  $\tau$  or  $T_{\text{brk}}$ , as appropriate, in the abscissa. Apparently one relation extrapolates into the other.

(A color version of this figure is available in the online journal.)

obtained a correlation between the spectral lag  $\tau$  and rest-frame jet-break time  $\tau_j$  given by

$$\tau_j = 28_{-11}^{+18} \left( \frac{\tau}{1\text{s}} \right)^{0.89 \pm 0.12} \text{ days}, \quad (10)$$

using a sample of seven BATSE GRBs. Another correlation between prompt and afterglow quantities was recently obtained by Margutti et al. (2012), who obtained a three-parameter correlation between the rest-frame isotropic energy in the prompt phase  $E_{\gamma,\text{iso}}$ , the peak of the prompt emission energy spectrum  $E_{\text{pk}}$ , and the X-ray energy emitted in the 0.3–10 keV observed energy band  $E_{X,\text{iso}}$  given by

$$E_{X,\text{iso}} \sim \frac{E_{\gamma,\text{iso}}}{E_{\text{pk}}^{3/4}}. \quad (11)$$

It was shown that this relation is robust and independent of the definition of  $E_{X,\text{iso}}$ . Moreover Margutti et al. (2012) and Bernardini et al. (2012) showed that this three-parameter relation is shared by both long and short GRBs and also claim that the physical origin of such a relation is related to the outflow Lorentz factor.

At this stage we do not intend to speculate on the possible physics underlying the correlations of Equations (7) and (8). Instead, we present a brief review of proposed explanations found in the literature. Then we conclude that, if indeed the underlying physics is common, as Figure 3 suggests, the apparently common origin of the two effects is basically kinematic.

In the case of the spectral-lag–luminosity relation, one possible explanation for the observed lags involves the spectral evolution during the prompt phase (Dermer 1998; Kocevski & Liang 2003; Ryde 2005) in which, due to cooling effects,  $E_{\text{pk}}$  shifts toward a lower energy band so that the temporal peak of the corresponding light curve will also shift to lower energies, thereby resulting in the observed lag. Another explanation for the spectral-lag–luminosity relation is based purely on kinematic effects (Salmonson 2000; Salmonson & Galama 2002; Ioka & Nakamura 2001; Dermer 2004; Shen et al. 2005; Lu et al. 2006), where the peak luminosity  $L_{\text{pk}}$  and spectral lag  $\tau$  depend on a single kinematic variable

$$D = \frac{1}{\Gamma(1 - \beta \cos \theta)(1 + z)}, \quad (12)$$



which represents the Doppler factor for ejecta in a jet, moving at an angle  $\theta$  from the line of sight with velocity  $\beta \equiv v/c$  at redshift  $z$ . This kinematic variable relates a proper timescale  $\tau$  in the GRB rest frame to the observed timescale  $t$  given by

$$t = \frac{\tau}{D}, \quad (13)$$

so that if the spectral lag is due to some decay timescale  $\Delta\tau$  in the GRB rest frame, then this will become  $\Delta t = \Delta\tau/D$  in the lab frame. Moreover, assuming a power-law spectrum with a low end of the form  $\phi(E) \propto E^{-\alpha}$ , where  $\alpha$  is the low-energy spectral index, Salmonson (2000) showed that the peak luminosity varies as

$$L_{\text{pk}} \propto D^{\alpha}, \quad (14)$$

with  $\alpha \approx 1$  (Preece et al. 1998), so that Equations (13) and (14) lead to the lag–luminosity relation. The same argument was used by Salmonson & Galama (2002) to explain their correlation in Equation (10), where in this case the jet-break time  $\tau_j \propto 1/D$ .

In this approach, the dependence of luminosities and observed timescales on the single variable  $D$  leads to the conclusion that the observed variety among GRBs has a kinematic origin, brought about through variation of the viewing angle  $\theta$  or the Lorentz factor  $\Gamma$  profile of the jet  $\Gamma$ , or both. So, for example, Salmonson (2000) showed that the lag–luminosity relation is due only to a variation in the line-of-sight  $\Gamma$  among bursts, with high  $\Gamma$  bursts having smaller spectral lags and low  $\Gamma$  bursts exhibiting longer ones. On the other hand, Ioka & Nakamura (2001) showed that the lag–luminosity relation can be explained by variation in the observer angle,  $\theta_v$ , from the axis of the jet, using a simple jet in which  $\Gamma = \text{const.}$  for  $\theta < \theta_j$ , and zero emission for  $\theta > \theta_j$ , where  $\theta_j$  is the opening angle of the jet. In this case the lags arise due to the path difference between the near and far edges of the emitting region such that bright (dim) bursts with short (long) spectral lags correspond to a small (large) viewing angle.

An explanation for the anti-correlation between the duration of the intrinsic plateau phase of the GRB light curve and X-Ray luminosity has been proposed by Dall’Osso (2010) using a model in which energy from a long-lived central engine is continuously injected to balance the radiative losses. These radiative losses will be stronger for higher luminosity, thus leading to shorter plateaus. Another explanation, which is based on the kinematic effect discussed above, was proposed by Eichler & Granot (2006), who claimed that the flat (or sometimes slightly rising) decay phase of the afterglow light curve results from the combination of the decaying tail of the prompt emission and early afterglow observed at viewing angles slightly outside the edge of the jet. For such “offset” viewing angles the afterglow flux initially rises at early times when the beaming of radiation away from the line of sight gradually decreases, then rounds off as the beaming cone expands to include the line of sight, and finally joins the familiar decaying light curve.

Clearly, the relations given by Equations (7)–(9) call for further analysis with larger data sets to determine whether the indices and normalization of these relations are indeed consistent with those presented above. Since the relations in Equations (7) and (8) correspond to the prompt and afterglow phases of the GRB evolution, the similarity of their power-law indices and normalizations (they extrapolate into each

other in Figure 3) is an indication that a common process, probably a kinematic one, is responsible for the observed spectral lags and the shallow decay phase of the afterglow light curve. As discussed above, both these relations were attributed individually (Ioka & Nakamura 2001; Eichler & Granot 2006) to the same kinematic process, namely, viewing the GRB jets at “off-beam” lines of sight. The results presented in this paper are in accordance with this explanation.

We acknowledge useful discussions with Takanori Sakamoto. J.S. gratefully acknowledges financial support from the University of Malta during his visit at NASA-GSFC.

## REFERENCES

- Amati, L., Frontera, F., & Guidorzi, C. 2009, *A&A*, **508**, 173  
 Band, D. L. 1997, *ApJ*, **486**, 928  
 Band, D. L., Matteson, J., Ford, L., et al. 1993, *ApJ*, **413**, 281  
 Bernardini, M. G., Margutti, R., Zaninoni, E., & Chincarini, G. 2012, *MNRAS*, **425**, 1199  
 Cannizzo, J. K., Troja, E., & Gehrels, N. 2011, *ApJ*, **734**, 35  
 D’Agostini, G. 2005, arXiv:physics/0511182  
 Dainotti, M. G., Cardone, V. F., & Capozziello, S. 2008, *MNRAS*, **391**, L79  
 Dainotti, M. G., Cardone, V. F., Capozziello, S., Ostrowski, M., & Willingale, R. 2011a, *ApJ*, **730**, 135  
 Dainotti, M. G., Ostrowski, M., & Willingale, R. 2011b, *MNRAS*, **418**, 2202  
 Dainotti, M. G., Willingale, R., Capozziello, S., Cardone, V. F., & Ostrowski, M. 2010, *ApJ*, **722**, L215  
 Dall’Osso, S., Stratta, G., Guetta, D., et al. 2011, *A&A*, **526**, A121  
 Dermer, C. D. 1998, *ApJ*, **501**, L157  
 Dermer, C. D. 2004, *ApJ*, **614**, 284  
 Eichler, D., & Granot, J. 2006, *ApJ*, **641**, L5  
 Evans, P., Beardmore, A. P., Page, K. L., et al. 2009, *MNRAS*, **397**, 1177  
 Gehrels, N., Norris, J. P., Barthelmy, S. D., et al. 2006, *Nature*, **444**, 1044  
 Ghirlanda, G., Ghisellini, G., & Firmani, C. 2006, *New J. Phys.*, **8**, 123  
 Hakkila, J., Giblin, T. W., Norris, J. P., Fragile, P. C., & Bonnell, J. T. 2008, *ApJ*, **677**, L81  
 Hakkila, J., Giblin, T. W., Young, K. C., et al. 2007, *ApJS*, **169**, 62  
 Ioka, K., & Nakamura, T. 2001, *ApJ*, **554**, L163  
 Kocevski, D., & Liang, E. 2003, *ApJ*, **594**, 385  
 Lu, R.-J., Qin, Y.-P., Zhang, Z.-B., & Yi, T.-F. 2006, *MNRAS*, **367**, 275  
 Margutti, R., Zaninoni, E., Bernardini, M. G., et al. 2012, arXiv:1203.1059v1  
 Norris, J. P. 2002, *ApJ*, **579**, 386  
 Norris, J. P., & Bonnell, J. T. 2006, *A&A*, **643**, 266  
 Norris, J. P., Marani, G. F., & Bonnell, J. T. 2000, *ApJ*, **534**, 248  
 Nousek, J. A., Kouveliotou, C., Grupe, D., et al. 2000, *ApJ*, **642**, 389  
 Piran, T. 2004, *Rev. Mod. Phys.*, **76**, 1143  
 Preece, R. D., Pendleton, G. N., Briggs, M. S., et al. 1998, *ApJ*, **496**, 849  
 Qi, S., & Lu, T. 2010, *ApJ*, **717**, 1274  
 Riechart, D. E., Lamb, D. Q., Fenimore, E. E., Ramirez-Ruiz, E., & Cline, T. L. 2001, *ApJ*, **552**, 57  
 Ryde, F. 2005, *A&A*, **429**, 869  
 Sakamoto, T., Sato, G., Barbier, L., et al. 2009, *ApJ*, **693**, 922  
 Salmonson, J. D. 2000, *ApJ*, **544**, L115  
 Salmonson, J. D., & Galama, T. J. 2002, *ApJ*, **569**, 682  
 Schaefer, B. E. 2003, *ApJ*, **583**, L67  
 Schaefer, B. E. 2004, *ApJ*, **602**, 306  
 Schaefer, B. E. 2007, *ApJ*, **660**, 16  
 Shen, R.-F., Song, L.-M., & Li, Z. 2005, *MNRAS*, **362**, 59  
 Stamatikos, M., Ukwatta, T. N., Sakamoto, T., et al. 2008, in AIP Conf. Ser. 1000, Gamma-ray Bursts 2007, ed. M. Galassi, D. Palmer, & E. Fenimore (Melville, NY: AIP), 137  
 Stratta, G., Guetta, D., D’Elia, V., et al. 2010, in AIP Conf. Proc. 1279, Deciphering the Ancient Universe with Gamma-ray Bursts, ed. N. Kawai & S. Nagataki (Melville, NY: AIP), 421  
 Ukwatta, T. N., Dhuga, K. S., Stamatikos, M., et al. 2012, *MNRAS*, **419**, 614  
 Ukwatta, T. N., Stamatikos, M., Dhuga, K. S., et al. 2010, *ApJ*, **711**, 1073  
 Wang, F.-Y., Qi, S., & Dai, Z. -G. 2011, *MNRAS*, **415**, 3423  
 Willingale, R. W., O’Brien, P. T., Osborne, J. P., et al. 2007, *ApJ*, **662**, 1093